International Journal of Environmental Sciences
ISSN: 2229-7359
Vol. 11 No. 23s, 2025
https://theaspd.com/index.php

Ph-Responsive Gelatin/Peg/Zno Hydrogel Matrix for Controlled Release of Cephalexin: Swelling Behavior, Drug Kinetics, And Antimicrobial Efficacy

Ahmed Kadhim Hussien[1], Oraas Adnan Hatem[2]
[1,2] Department of Chemistry, College of Sciences,University of AL-Qadisiyah, Al-Qadisiyah, , Iraq.
Corresponding Author: **Oraas Adnan Hatem, E-mail:** oraas.adnan@qu.edu.iq

Abstract

This study presents the development and evaluation of a gelatin/polyethylene glycol/zinc oxide (Gel/PEG/ZnO) hydrogel matrix designed for controlled drug delivery applications. The hydrogel was synthesized through the physical blending of gelatin and PEG, followed by chemical crosslinking using glutaraldehyde and the incorporation of zinc oxide nanoparticles (ZnO) to enhance structural stability and antibacterial activity.

Swelling behavior was investigated under simulated gastric (SGF, pH 1.2) and intestinal (SIF, pH 6.8) conditions, revealing significant pH sensitivity. The hydrogel exhibited a maximum swelling percentage of 1450% in SIF and 680% in SGF, confirming its suitability for intestinal-targeted drug release. Cephalexin was loaded into the hydrogel matrix, and in vitro drug release studies indicated a sustained release profile, achieving 99.89% release in SIF over 24 hours. Kinetic modeling demonstrated the best fit with the Higuchi model, indicating a diffusion-controlled mechanism.

FTIR analysis confirmed successful polymer interaction and drug incorporation, while SEM imaging revealed morphological changes consistent with drug loading.

Antibacterial testing showed a 20 mm inhibition zone against Staphylococcus aureus, confirming the synergistic effect of ZnO and cephalexin. These findings suggest that the Gel/PEG/ZnO hydrogel is a promising candidate for pH-responsive, prolonged-release antibiotic delivery systems.

KeyWords: *Gelatin, polyethylene glycol (PEG), ZnO nanoparticles, controlled Drug delivery, Cephalexin.*

1 INTRODUCTION

Medical treatments have extended life and improved health since ancient times. Recently and soon, drug delivery will shift. Biomedical engineers have invented unique clinically employed technologies and aided in comprehending biological barriers to medication delivery, such as drug dispersion and circulation in the body and drug transport across tissues and cells[1].

Medical advancements in recent decades have come from controlled-release drug delivery devices. Pharmaceutical release is managed by these systems to reduce administration frequency and maintain efficacy. Controlled-release formulations can deliver the drug slowly, zero-order, or first-order, or provide a fast initial dose followed by a controlled release time[2].

Nanotechnology is one of the best ways to achieve this goal by developing nanostructures with better medication delivery capabilities. Nanotechnology's molecular-level manipulation of material properties has garnered attention because it enables the development of very effective and accurate drug carriers. In addition to medication delivery, these nanostructures are being studied for electronics, magnetic materials, optoelectronics, catalysis, and biomedical engineering. Targeted ways provide medications to sick cells using various strategies. These systems use cell surface receptors, pH gradients, and magnetic fields to optimize drug accumulation at the targeted region and reduce systemic exposure. Medication delivery systems require interdisciplinary expertise from pharmaceutical sciences, material science, bioengineering, and medical research. Scientists and researchers are constantly improving these systems to improve patient comfort, toxicity, and pharmaceutical efficacy[3 -9].

Protein-based polymers can be used in biopolymer devices for drug delivery due to their high drug binding, low cytotoxicity, biodegradability, and abundance. Specific cells readily absorb them. Because polypeptide main sequences contain functional groups, their protein structure allows surface modifications. The gut digests proteins easily[10].

Collagen-derived gelatin is biocompatible and biodegradable. After biodegradation, low-antigenicity animal metabolites create collagen. Environmental variables including pH, temperature, and biological stimulation affect gelatin. Gelatin capsules offer medicine since 1834. Increase medication consumption, control dosage, and improve use and storage. As nanomaterials progressed, hydrogels, gelatin

nanospheres, nanogels, and nanofibers replaced small capsules. Drug delivery carriers made of gelatin are common in the pharmaceutical industry[11, 12].

2 MATERIALS AND METHODS

2.1 Materials

Cephalexin ($C_{16}H_{17}N_3O_4S{\cdot}H_2O$, MWT = 365.41 g/mol) was procured from Calyx Chemicals Pharmaceuticals Ltd (India). Soy Protein Isolation from Shandong Wonderful Biotech Co., Gelatin was procured from Geltech Co., polyethylene glycol (PEG) from Jungwoo Co., and ZnO nanoparticles from NHTNM Co. Glutaraldehyde, Central Drug House Co., Hydrochloric Acid (HCl), J.K. Baker, Netherlands, Sodium Hydroxide Meru Chem Pvt. Ltd. Utilize deionized water for the preparation of all solutions.

2.2 Gelatin Hydrogel Polymeric matrix preparation

To formulate the gelatin-based hydrogel, one gram of gelatin was initially dissolved in ten milliliters of deionized water. An equivalent mass of polyethylene glycol (PEG) was then gradually incorporated, and the mixture was stirred continuously for twenty minutes to achieve homogeneity. The pH of the solution was raised to approximately 11 using a 5 M sodium hydroxide solution to promote gelatin solubilization and enhance polymer compatibility. Subsequently, 0.1 grams of zinc oxide (ZnO) nanoparticles were introduced and uniformly dispersed through sustained agitation. Glutaraldehyde (1 mL) was then added dropwise to initiate crosslinking, and stirring was maintained for an additional hour to allow sufficient time for covalent bonding between the functional moieties of gelatin and PEG. The final solution was cast into a Petri dish and left at ambient temperature until full gelation and drying occurred. The same process was repeated using reduced gelatin quantities (0.7 g and 0.3 g) to generate hydrogel variants exhibiting differing swelling capacities. Among these, the mixture comprising 0.7 g gelatin, 0.3 g PEG, and 0.5 mL glutaraldehyde produced the most structurally consistent and stable hydrogel.

2.3 Drug-loaded Hydrogel Polymeric matrix preparation

A quantity of 0.01 g of cephalexin was accurately weighed using a precision electronic balance and incorporated into the components of the hydrogel polymeric matrixes . The mixture was stirred thoroughly at room temperature for 30 minutes to ensure uniform drug distribution. Subsequently, the formulation was cast into Petri dishes and left to dry at ambient conditions. The same steps were followed for the gelatin-based hydrogel polymeric matrix.

2.4 Preparation of Simulated Gastric Fluid (SGF):

Based on data obtained from the Encyclopedia of Medicines, a non-enzymatic simulated gastric fluid (SGF) was prepared. Two grams of sodium chloride (NaCl) were dissolved in 500 mL of distilled water under continuous stirring. Subsequently, 10 mL of concentrated hydrochloric acid (HCl) was added, and the volume was adjusted to 1000 mL with distilled water. The final solution simulates the acidic conditions of gastric fluid, with a target pH of approximately 1.2.

2.5 Preparation of Simulated Intestinal Fluid (SIF):

Following the guidelines of the American Academy of Dermatology, a non-enzymatic simulated intestinal fluid (SIF) was prepared. Initially, 8.6 grams of monopotassium phosphate (KH_2PO_4) were dissolved in 250 mL of purified water. Subsequently, 190 mL of a 0.2 M sodium hydroxide (NaOH) solution was added, and the total volume was adjusted to 1000 mL with purified water. This buffer solution mimics the pH and ionic environment of intestinal fluid, typically around pH 6.8.

2.6 Analysis of the Swelling Ratio of the Prepared Polymeric Matrix

The swelling behaviour was assessed by submerging the laboratory-synthesized hydrogel samples in water solutions at ambient temperature (27 °C).After 24 hours, the samples were extracted and delicately wiped using filter paper to remove excess surface moisture. The swelling ratio of each hydrogel was then determined using the following formula [13-15]:

$$\mathbf{SR} = \frac{\mathbf{ws - wd}}{\mathbf{wd}} \times \mathbf{100\%} \quad \text{..... (1)}$$

Where (SR) represents the swelling ratio of the hydrogel sample, Wd represents the weight of the dry sample, while Ws denotes the swollen weight .

2.7 Assessment of Drug Release Percentage from the Hydrogel Polymeric Matrix

Cephalexin release from the hydrogel matrices was evaluated by immersing the samples in simulated gastric and intestinal fluids under stable laboratory conditions. At regular time points, aliquots of the surrounding medium were collected and analyzed using UV-Visible spectrophotometry, measuring absorbance at 261 nm, the drug's specific wavelength. This procedure enabled the calculation of cumulative drug release, expressed as a percentage relative to the initially loaded amount, providing a clear profile of the release behavior over time.The percentage of drug released was calculated using the following equation [16,17]:

$$\textbf{Release \%} = \frac{\textbf{concentration of drug released with Time}}{\textbf{concentration of drug loaded}} \times \textbf{100 \% …… (2)}$$

2.8 Characterizations

2.8.1 FTIR Measurement

FTIR spectroscopy was employed to investigate the molecular composition of the unloaded polymeric matrix and its cephalexin-loaded counterpart. This analysis aimed to detect characteristic functional groups and examine any interactions between the drug and matrix components. For measurement, each sample was blended with finely ground potassium bromide (KBr) and compressed into transparent pellets. Infrared spectra were collected within the range of 600 to 4000 cm^{-1}, allowing for detailed evaluation of the relevant vibrational features.

2.8.2 SEM Measurement

Scanning electron microscopy (SEM) was applied to analyze the surface architecture and morphological features of the polymeric matrix prior to and following cephalexin incorporation. This method provided high-resolution visual data that helped identify physical alterations linked to drug loading, including shifts in surface texture, particle size distribution, and overall structural consistency.

2.8.3 Antibacterial Tests

The antibacterial properties of the hydrogel formulations were evaluated through the agar well diffusion assay against two bacterial strains: Staphylococcus aureus (Gram-positive) and Escherichia coli (Gram-negative). Bacterial suspensions were prepared using sterile saline and adjusted to a final concentration of 1.5×10^8 CFU/mL. Turbidity was standardized using a 0.5 McFarland reference to ensure reproducibility. Each bacterial culture was uniformly spread over Mueller-Hinton agar plates with sterile swabs. Wells were then filled with the hydrogel test formulations, and the plates were incubated at 37 °C for 24 hours. After incubation, the diameter of the clear zones around each well was measured in millimeters to determine the extent of bacterial growth inhibition, thereby indicating the antimicrobial effectiveness of each sample.

3 RESULTS AND DISCUSSION

3.1 FTIR Analysis and Discussion of Gel/PEG/ZnO Polymeric Matrix Before and After Cephalexin Loading

The gelatin/PEG/ZnO nanoparticle-based hydrogel system, chemically crosslinked using glutaraldehyde, was analyzed using Fourier-transform infrared (FTIR) spectroscopy to investigate structural features and drug incorporation behavior before and after the loading of cephalexin, as shown in Figures 1 and 2. The FTIR spectrum of the unloaded formulation (G1) revealed a broad and intense absorption band around 3290.56 cm^{-1}, corresponding to O–H and N–H stretching vibrations, which are indicative of extensive intermolecular hydrogen bonding within the polymer network composed of gelatin and PEG [18,19]. In the region 2937.59–2881.65 cm^{-1}, characteristic C–H stretching vibrations of methylene groups were observed, attributable to the PEG chaians [20].

Gelatin protein backbone was confirmed by the presence of amide I and amide II bands, with a prominent peak at 1651.07 cm^{-1} corresponding to C=O stretching (amide I) and another at 1539.20 cm^{-1} attributed to N–H bending (amide II), both typical of collagen-derived biopolymers [21, 22]. These bands reflect the integrity of gelatin's secondary structure within the hydrogel. Several additional peaks were present in the range 1200–600 cm^{-1}, which can be attributed to C–O stretching vibrations from PEG, Zn–O stretching , and other matrix-related interactions [23].Specifically, bands around 1145–1026 cm^{-1} relate to C–O–C ether vibrations , while absorption near 842.95 cm^{-1} and 690.86 cm^{-1} confirm the presence of Zn–O bonds, indicating the successful incorporation of ZnO nanoparticles into the hybrid network.

Following cephalexin incorporation (G2), significant spectral alterations were observed that clearly demonstrate the interaction between the drug and the hydrogel components. A distinct new absorption peak at 1766.80 cm^{-1} was identified, corresponding to the C=O stretching vibration of the β-lactam ring

in cephalexin. This confirms the successful integration of the drug into the polymer matrix. Additionally, a peak emerged at 1692.62 cm^{-1} , which likely represents additional carbonyl functionality from the carboxyl or β-lactam moieties of cephalexin. The amide I and II bands also showed slight increases in intensity , suggesting enhanced hydrogen bonding interactions between cephalexin and the matrix polymers, possibly involving gelatin amide groups and PEG hydroxyls.

In the fingerprint region (1200–600 cm^{-1}) , minor shifts and increased absorbance were detected, particularly between 1283.52 and 1030.27 cm^{-1} , which may be associated with C–N and C–O stretching vibrations of cephalexin engaged in hydrogen bonding or dipolar interactions with the matrix. Additionally, the Zn–O band at ~842 cm^{-1} remained consistent in position but slightly increased in intensity, while a new signal near 690.37 cm^{-1} may indicate interaction between cephalexin and ZnO nanoparticles. These modifications in the spectral profile point to intermolecular interactions, including hydrogen bonding, dipole–dipole forces, and possibly weak electrostatic attractions between cephalexin and the gelatin/PEG/ZnO nanocomposite.

gelatin/PEG/ZnO nanocomposite.

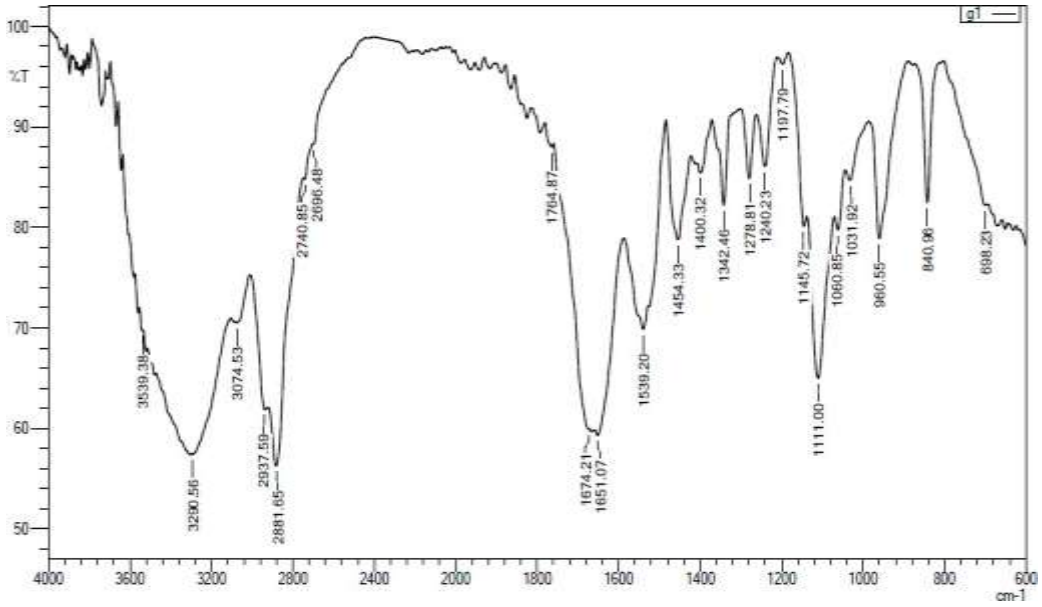

Figure (1) FTIR spectrum of the Gel /PEG/ZnO hydrogel matrix before cephalexin loading

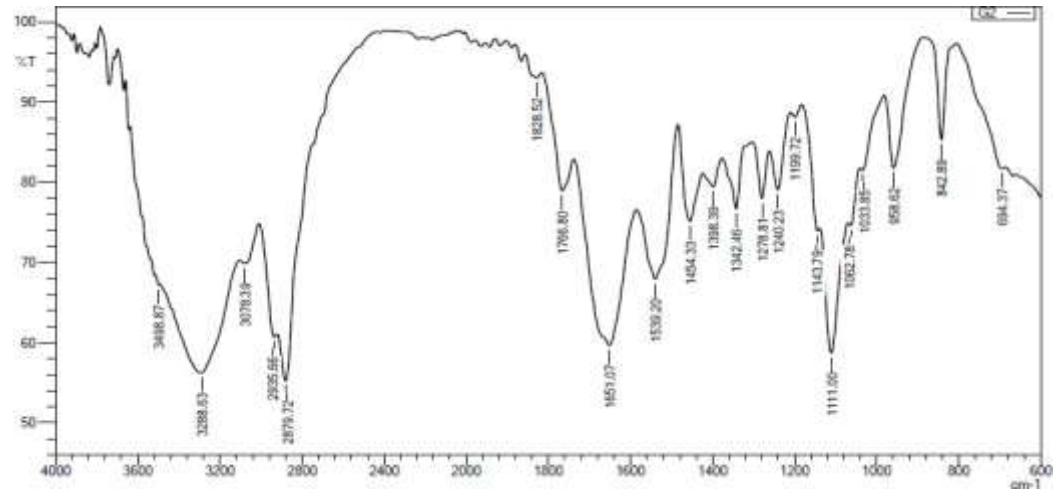

Figure (2) FTIR spectrum of the Gel/PEG/ZnO hydrogel matrix after cephalexin loading.

3.2 Study of swelling ratios of prepared polymeric compositions

The swelling properties of the prepared polymeric nanocomposite hydrogels were evaluated by immersing the samples in distilled water for 24 hours under ambient conditions. Swelling ratio serves as a crucial

parameter in assessing the hydrogel ability to absorb water and is directly related to its potential as a controlled drug delivery system. The 0.3PEG:0.7Gelatin hydrogel reached a maximum swelling ratio of 1132%, while the 1PEG:1Gelatin and 0.7PEG:0.3Gelatin compositions recorded 738% and 233%, respectively. This enhanced swelling behavior of gelatin-based hydrogels, as shown in Figure 3, can be attributed to gelatin intrinsic hydrophilic nature and greater capacity for hydrogen bonding with water molecules. The presence of additional polar functional groups in gelatin, such as amide and carboxylic moieties, promotes greater water absorption .

The superior swelling performance of gelatin-based matrices indicates their potential advantage in drug delivery applications where rapid hydration and high fluid uptake are desirable. Moreover, the data underscore the tunability of hydrogel properties through compositional modifications, offering design flexibility for targeted biomedical applications.

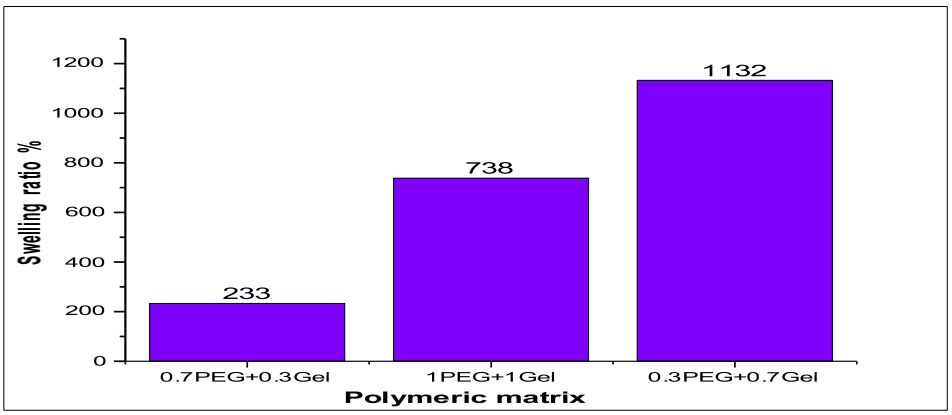

Figures (3) Swelling ratio of Gel/PEG/ZnO

3.3 Study the effect of the crosslinking agent on the swelling ratio of the polymeric matrix

The swelling characteristics of gelatin samples were examined by incorporating varying quantities of glutaraldehyde. The samples lacking a crosslinking agent exhibited no swelling and instead disintegrated in the water solution. This results from the elevated solubility of gelatin, and PEG. Consequently, a crosslinking agent is essential in any polymeric matrix comprising gelatin to improve their mechanical characteristics and diminish their solubility in aqueous solutions. It was noted that expanding the quantity of crosslinker rendered the samples more stiff and accelerated their aggregation; however, the swelling ratios diminished. This behaviour is natural, as the elevated crosslink density obstructs water infiltration into the polymeric matrix [24,25]. The findings indicated that the ideal added volume was 0.5 ml for gelatin matrices, at which the samples attained the highest swelling ratio. This demonstrates that the crosslinking forces did not impede swelling, while the dimensional stability and integrity of the samples were preserved, as illustrated in Figure (4) .

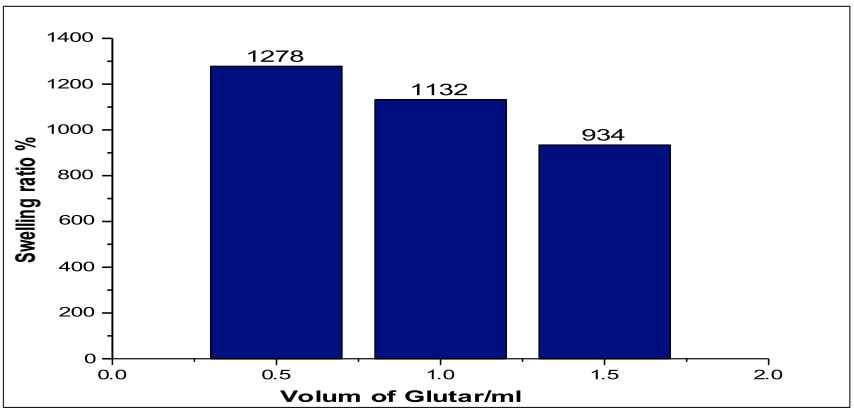

Figure (4) Impact of crosslinking agent on the swelling ratios of polymeric matrix

3.4 Swelling Behavior of Polymeric Matrices in Simulated Gastrointestinal Conditions

To evaluate the pH-responsive behavior of the synthesized polymeric hydrogels, the swelling performance of Gelatin/PEG (Gel/PEG) matrices was assessed in simulated gastric fluid (SGF, pH ~1.2) and simulated

intestinal fluid (SIF, pH ~6.8). These media were selected to mimic the physiological conditions of the human gastrointestinal tract and assess the suitability of the hydrogels for oral drug delivery applications. The results, presented in Figure (5), reveal that the hydrogel systems exhibited marked pH-sensitive swelling , confirming their responsiveness to environmental pH variations.

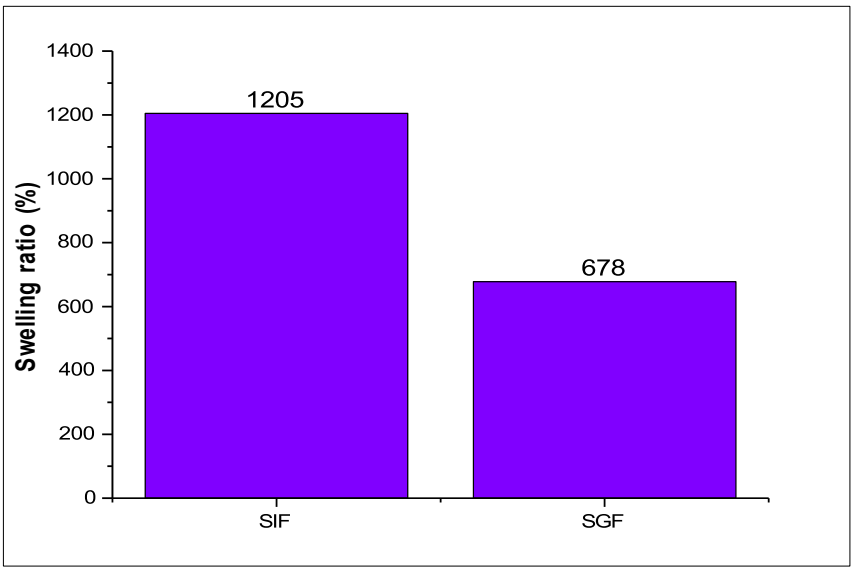

Figure (5) Swelling ratios of polymeric matrix in simulated gastric fluid and intestinal fluid

The Gel/PEG matrix displayed a considerably hight swelling response across both media. In SGF, the swelling ratio reached 678%, and in SIF, it increased further to an impressive 1205%. The enhanced swelling behavior of the gelatin-based system is attributable to gelatin's highly hydrophilic nature and the abundance of ionizable functional groups (e.g., –COOH and $–NH_2$), which exhibit strong hydration potential. Furthermore, gelatin flexible polymer chains and less compact network architecture allow for more efficient solvent penetration and matrix expansion. The underlying mechanism of swelling in hydrogel involves the diffusion of solvent molecules into the polymeric network, where they interact with hydrophilic moieties on the polymer chains. Rather than dissolving completely, the hydrogel undergoes a phase transition into a gel-like state characterized by partial chain mobility and significant volumetric expansion [26].These findings demonstrate that Gel/PEG system is capable of pH-triggered swelling, an essential feature for site-specific drug delivery in the gastrointestinal tract. positioning it as a more promising candidate for applications requiring high fluid uptake and rapid drug release in the intestinal environment.

3.5 Kinetic study of polymeric matrix swelling

The swelling behavior of hydrogel-based drug delivery systems is a critical determinant of their performance, as it directly influences both the rate of drug release and the degradation kinetics of the polymer matrix. The absorption of water by hydrogels causes them to swell, which facilitates drug diffusion through the hydrated polymer network. This process is closely governed by the physicochemical properties of the hydrogel, including crosslink density, porosity, and hydrophilicity, as well as environmental conditions such as pH and temperature.

To gain a deeper understanding of the water diffusion mechanisms in the prepared hydrogel matrices, kinetic modeling was employed. The time-dependent swelling process was evaluated using empirical models, including the power law model (Korsmeyer–Peppas equation) and the second-order swelling kinetic model.

The first model applied was a semi-empirical power law expression used to describe water diffusion into the hydrogel network[25]:

$$Ln\frac{Wt}{Wmax} = Ln\,k + n\,Ln\,t \quad \ldots\ldots(3)$$

Where:

Wt: is the amount of water absorbed at time t

W_{max}: is the equilibrium water uptake (maximum swelling),

K: is the swelling rate constant,
n: is the diffusional exponent, which characterizes the mode of water transport and provides insight into the underlying diffusion mechanism:
$n \leq 0.5$: Fickian diffusion, governed predominantly by solvent diffusion with minimal polymer relaxation.
$0.5 < n < 1$: Anomalous (non-Fickian) transport, involving a combination of diffusion and polymer relaxation.
$n = 1$: Case II transport, where the release is dominated by polymer chain relaxation rather than solvent diffusion.
This model is particularly suitable for analyzing initial swelling behavior and distinguishing between diffusion-limited and relaxation-controlled processes within the hydrogel matrix[26].
In addition to the power law model, a second-order kinetic model was employed to further evaluate the swelling dynamics, particularly for long-term behavior. The second-order swelling equation is expressed as[26,27]:

$$\frac{t}{W_t} = A + \frac{t}{W_\infty} \quad \text{.....(4)}$$

A is a constant defined by the following equation:

$$A = \frac{1}{kW_\infty^2} \quad \text{.....(5)}$$

Plotting the relationship between t/W_t and time yields a straight line with a slope of $1/W_\infty$. The constant k can be ascertained from the intercept of the linear equation, as per Equation (3.4).
This model assumes that swelling is controlled by the availability of free water and the polymer's ability to absorb it over time [28,29].

3.6 Swelling Kinetic Study of Gel/PEG/ZnO polymeric Matrix

A detailed kinetic study was conducted to assess the swelling behavior of the gelatin/polyethylene glycol hydrogel matrix loaded with ZnO nanoparticles. Over a period of 390 minutes, the swelling ratio was quantified at defined time intervals to evaluate the hydrogel fluid uptake capacity and hydration dynamics. The results are presented in Tables (1) and (2) and visualized in Figures (6) and (7)
The swelling ratio increased progressively over time, reaching a maximum of 1205.37% at 390 minutes , indicating a highly absorbent hydrogel structure with considerable swelling potential. These high values are consistent with gelatin's strong hydrophilic character and the open network structure of the matrix, which enables substantial solvent diffusion.
To further understand the kinetic mechanism governing this behavior, the experimental data were fitted to both first-order(Korsmeyer–Peppas power law model) and second-order swelling models, and the corresponding rate constants and regression coefficients (R2) were determined (Table 3.4). The first-order kinetic model produced a regression coefficient of R2 = 0.96873 with a rate constant of 0.003 min^{-1}, indicating a strong linear relationship and good model fit. In contrast, the second-order model yielded a much lower R2 value of 0.65122, suggesting that it does not adequately describe the swelling dynamics of the Gel/PEG system.
The swelling mechanism evaluated using the Korsmeyer–Peppas power law model yielded a diffusional exponent (n) value of 1.00915, this value is nearly equivalent to the theoretical threshold for Case II transport (n = 1) [30-31], implying that the swelling process in the Gel/PEG/ZnO matrix is dominated not by diffusion alone, but by polymer chain relaxation dynamics. This mechanism is typical of hydrophilic polymer systems that undergo substantial volumetric expansion, where solvent uptake leads to a time-independent, constant-rate swelling phase.

Table (1) Swelling ratios, swelling degree and water content values of the Gel/PEG polymeric matrix

Time	Wt	swelling ratio	swelling degree Dh	water content	First order		second order
		(Ws-Wd)/ Wd*100	wet weight/dry weight	Ws-Wd	LN Time(Ln t)	LN(Wt/Wmax)	t/w

0	3.91						
30	8.64	120.97	2.21	4.73	3.40	-2.30	3.47
60	11.16	185.42	2.85	7.25	4.09	-1.87	5.38
90	15.35	292.58	3.93	11.44	4.50	-1.42	5.86
120	22.93	486.45	5.86	19.02	4.79	-0.91	5.23
150	29.21	647.06	7.47	25.30	5.01	-0.62	5.14
180	36.56	835.04	9.35	32.65	5.19	-0.37	4.92
240	42.93	997.95	10.98	39.02	5.48	-0.19	5.59
300	45.77	1070.59	11.71	41.86	5.70	-0.12	6.55
360	49.39	1163.17	12.63	45.48	5.89	-0.04	7.29
390	51.04	1205.37	13.05	47.13	5.97		

Table (2) Rate constants and Regression cofficient for the swelling kinetics of the Gel/PEG polymeric matrix

Model	Regression Coefficient R^2	Rate Constant
First Order	0.96873	0.003
Second Order	0.65122	1.43×10^{-5}

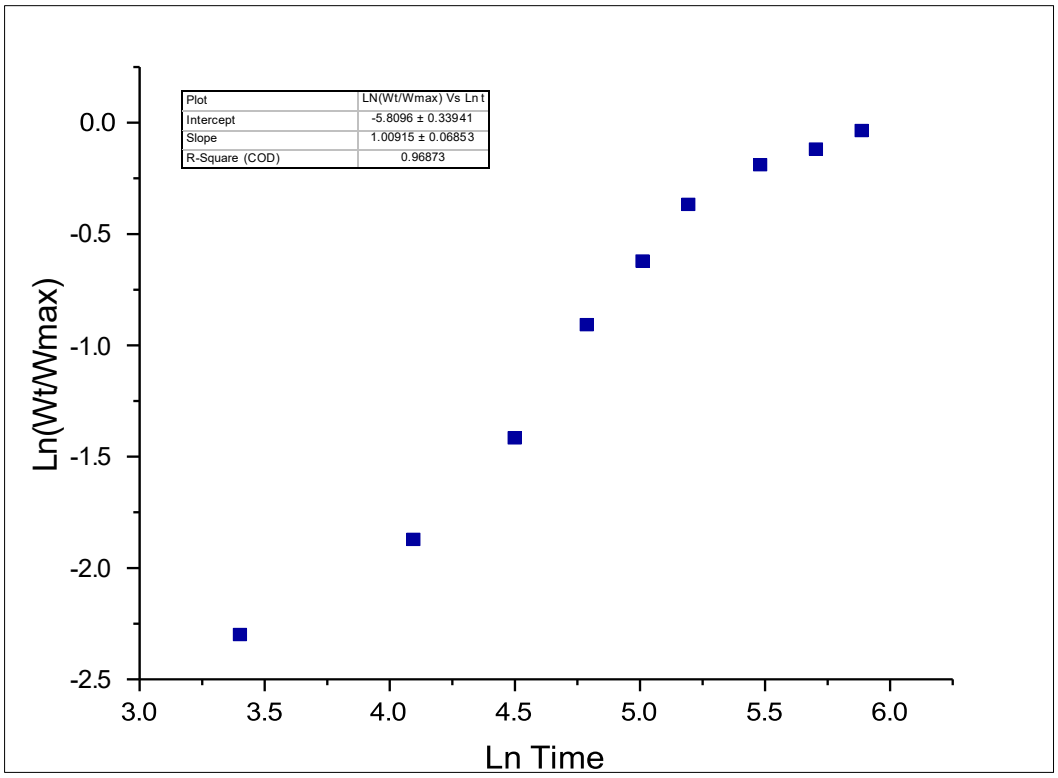

Figure (6) First-order kinetic model for the swelling behavior of the Gel/PEG polymeric matrix.

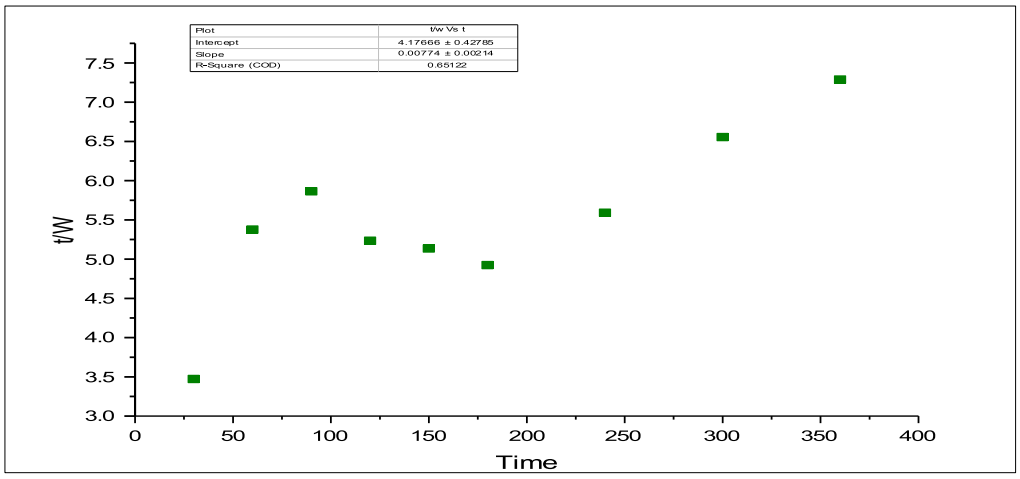

Figure (7)The second-order kinetic model for the swelling behavior of the Gel/PEG polymeric matrix

3.7 Kinetic Study for the Drug Release from the Polymeric Matrix

To elucidate the mechanism of drug release from the developed polymeric hydrogel matrices, kinetic modeling was employed using zero-order, first-order, and the Higuchi diffusion model. These models are commonly applied in pharmaceutical sciences to predict and interpret release profiles, optimize formulation parameters, and design controlled delivery systems.

The zero-order model assumes a constant drug release rate, independent of the concentration of the drug within the matrix. It is expressed by the following equation [32]:

$x = k_0$ t……(6)

X denotes the value of the drug release at time t , K is the zero-order release rate constant.

The first-order kinetic model describes a release mechanism in which the rate is proportional to the concentration of the drug remaining in the matrix.

$\ln C_t = \ln C_\circ - k_1 t$ …….(7)

C_0 is the initial drug concentration, Ct is the concentration at time t and k_1 is the first-order release rate constant.In this model, the release rate decreases exponentially with time, often observed in systems where diffusion is concentration-dependent.

Additionally, the Higuchi model was applied to assess whether the drug release was controlled by diffusion through a porous matrix. The simplified form of the Higuchi equation is given by :

f_t=Q= $k_H t^{1/2}$ ……(8)

Q is the cumulative amount of drug released at time t, and k_H is the Higuchi release constant.

3.8 Examine the drug release from the polymeric matrix

The in vitro release behavior of cephalexin from the synthesized polymeric hydrogels was investigated under physiologically relevant conditions, specifically in simulated intestinal fluid SIF and simulated gastric fluid SGF. The results revealed a significantly enhanced drug release profile from the Gel/PEG/ZnO matrix , as shown in Figures 8 and 9 .

In the Gel/PEG system, cephalexin release extended over a period of 24 hours, with a cumulative release of 99.89% in SIF and 44.24% in SGF. The reduced release observed in SGF is attributed to the acidic gastric environment, which can suppress swelling in hydrophilic matrices and influence drug solubility. . These results highlight the influence of matrix composition and network swelling properties on the drug release kinetics.The superior performance of the Gel/PEG matrix is associated with its higher swelling capacity, particularly under neutral to mildly basic conditions such as those simulated in SIF. Enhanced water uptake promotes polymer chain relaxation and facilitates diffusion of the encapsulated drug, resulting in nearly complete release.

A consistent trend was observed in matrix, with drug release efficiency being lower in SGF than in SIF. This behavior confirms that the hydrogel matrices exhibit pH-sensitive characteristics. The acidic pH of SGF induces contraction of the polymer network or protonation of functional groups, limiting matrix expansion and drug diffusion. In contrast, the more alkaline environment of SIF promotes matrix relaxation, increased porosity, and higher drug mobility [33, 34].

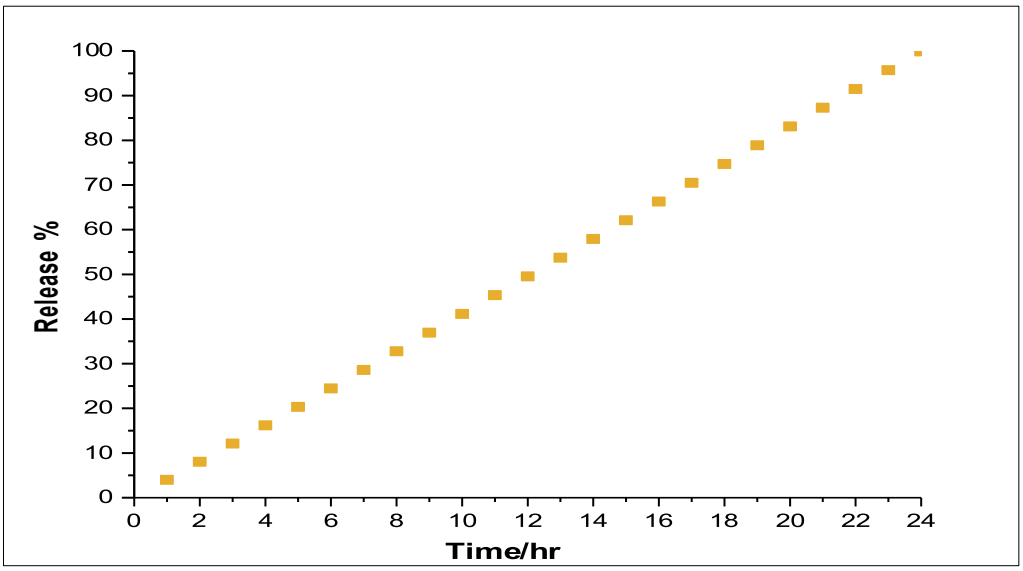

Figure (8)Release ratio of Gel/PEG-encapsulated cephalexin in SIF

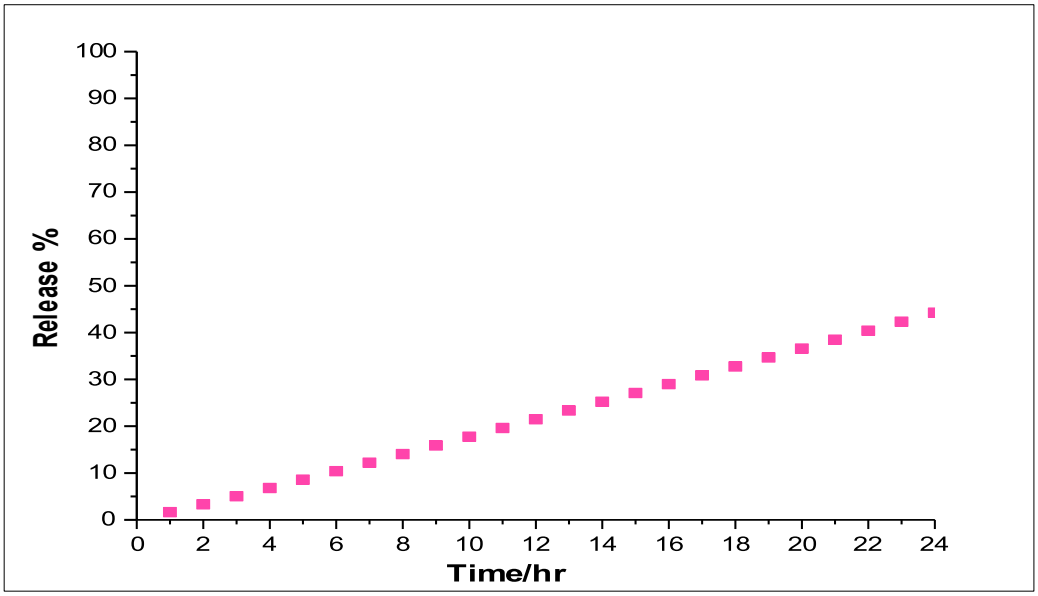

Figure (9)Release ratio of Gel/PEG-encapsulated cephalexin in SGF

3.9 Mechanism of Drug Release from the Polymeric Matrix

The primary mechanism governing drug release from the synthesized polymeric hydrogels in this study is diffusion-controlled transport. In such systems, drug molecules migrate from within the polymeric network into the surrounding release medium through a concentration gradient. This type of mechanism is particularly relevant for hydrogel-based delivery systems, where the polymer matrix acts as a physical barrier that modulates the rate and extent of drug release.

Diffusion occurs as the active compound moves through the hydrated, three-dimensional polymer structure, navigating between polymer chains that form the structural framework of the hydrogel. These polymer chains inherently limit the mobility of the drug due to physical entrapment, steric hindrance,

and intermolecular interactions. As the matrix becomes hydrated, it swells and expands, creating aqueous channels that facilitate molecular diffusion toward the external environment.

Although swelling and matrix erosion are often concurrent processes in hydrogel-based systems, the drug release mechanism in the current study was predominantly swelling-controlled diffusion, with erosion being excluded. This conclusion is supported by post-release observations confirming that the polymeric matrices retained their structural integrity throughout the release period. No significant disintegration or fragmentation was observed, indicating that matrix erosion did not contribute to the release mechanism. In this formulation strategy, the drug was uniformly dispersed within the polymer network, forming a homogeneous matrix system. Upon exposure to the release medium, the matrix absorbed fluid and swelled, which in turn facilitated drug diffusion through the swollen hydrogel network. As illustrated in Figure 10, the drug release process can be described as a two-step mechanism: initial swelling of the hydrogel followed by diffusion of the drug from the interior of the matrix into the external environment [35].

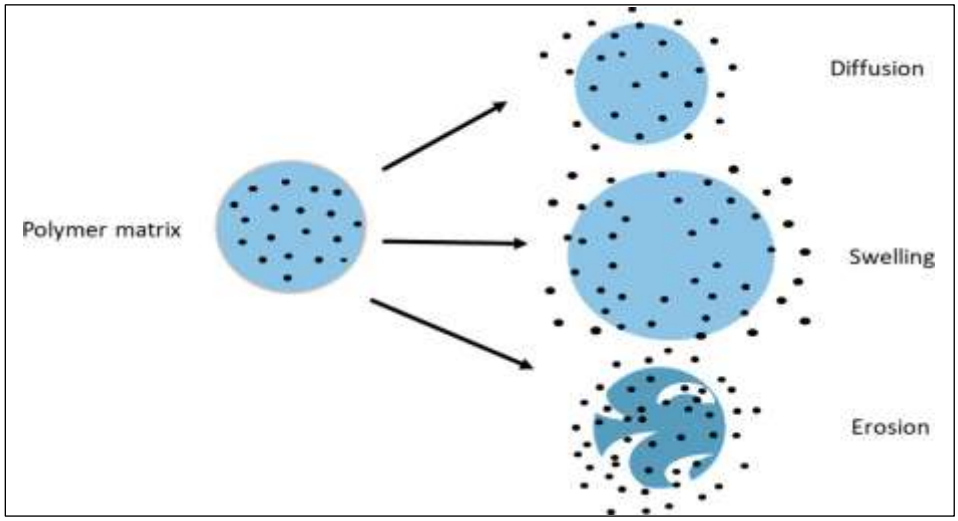

Figure (10) potential drug release mechanisms by diffusion, swelling, and erosion of the polymeric matrix[35]

3.10 Kinetic Analysis of Drug Release from the Polymeric Matrix

The release kinetics of cephalexin from the Gel/PEG polymeric matrix were systematically evaluated in both simulated intestinal fluid (SIF) and simulated gastric fluid (SGF). Tables 3 through 5 summarize the kinetic parameters calculated using three established models zero-order, first-order, and Higuchi while Figures 11 through 16 present the corresponding release profiles.

In SIF, the Gel/PEG/ZnO matrix exhibited an extended and nearly complete drug release, reaching a cumulative percentage of 99.89% within 24 hours. Among the applied models, the Higuchi model demonstrated the strongest correlation ($R2 = 0.812$) with a diffusion constant (k_H) of 0.0466, indicating that diffusion through the hydrated matrix dominated the release process. The zero-order and first-order models provided lower correlation coefficients of 0.665 and 0.637, respectively, suggesting that the release rate was neither strictly constant nor directly dependent on drug concentration remaining in the matrix. The superior alignment with the Higuchi model implies that cephalexin release from the Gel/PEG/ZnO system is predominantly governed by a diffusion-controlled mechanism. This behavior is typical of hydrophilic matrices, where drug molecules migrate through the swollen polymeric network into the external environment. The consistent release rate per hour (~4.2 ppm/h) throughout the 24 hour period supports the sustained and controlled release characteristics of the system.

In SGF, the matrix demonstrated a lower yet substantial release percentage of 44.24% over the same duration. Notably, the Higuchi model again exhibited the best fit, with a correlation coefficient (R2) of 0.924 and a rate constant (k_H) of 0.066. This finding is indicative of diffusion-based release behavior even under acidic conditions, although at a slower rate due to reduced matrix swelling. The zero-order and first-order models yielded slightly lower correlation values ($R2 = 0.817$ and 0.801, respectively), reinforcing the observation that release was primarily diffusion-controlled rather than erosion- or degradation-driven. The results indicate that Gel/PEG hydrogels are highly responsive to environmental pH, with a significantly enhanced drug release profile in intestinal conditions. The strong correlation with the Higuchi model across both pH environments supports the hypothesis that drug release occurs through a

swelling–diffusion mechanism. Furthermore, the high release efficiency and kinetic predictability of the Gel/PEG/ZnO matrix position it as a promising candidate for the development of sustained oral drug delivery systems.

Table (3) Rate constants and Registration coefficients values for the release kinetics of cephalexin in Gel/PEG polymeric matrix in different media

Medium	Zero Order		First Order		**Higuchi Model**	
	R2	K_0	R2	K_1	R2	K_H
SIF	0.665	0.0061	0.637	0.00006	0.812	0.0466
SGF	0.817	0.0098	0.801	0.00009	0.924	0.066

Table (4) Kinetic Parameters of Cephalexin Release from Gel/PEG Matrix in SIF

Time	**Cumulative Drug Release (ppm)**	**Amount Released per Hour**	**Release%**	**First Order**		**Higuchi**
		Qt	(Ct/Ci)*100%	Ci/(Ci-Ct)	Ln Ci/(Ci-Ct)	t^1/2
1	3.99	3.99	3.99	1.04155817	0.040717833	1
2	8.03	4.04	8.03	1.04210088	0.041238748	1.414213562
3	12.11	4.08	12.11	1.04253545		1.732050808
4	16.2	4.09	16.2	1.04264415	0.041759934	2
5	20.31	4.11	20.31	1.04286161	0.041968485	2.236067977
6	24.45	4.14	24.45	1.04318798	0.042281392	2.449489743
7	28.6	4.15	28.6	1.04329682	0.042385716	2.645751311
8	32.77	4.17	32.77	1.04351456	0.042594398	2.828427125
9	36.95	4.18	36.95	1.04362346	0.042698755	3
10	41.14	4.19	41.14	1.04373239	0.042803122	3.16227766
11	45.33	4.19	45.33	1.04373239	0.042803122	3.31662479
12	49.52	4.19	49.52	1.04373239	0.042803122	3.464101615
13	53.71	4.19	53.71	1.04373239	0.042803122	3.605551275
14	57.9	4.19	57.9	1.04373239	0.042803122	3.741657387
15	62.09	4.19	62.09	1.04373239	0.042803122	3.872983346
16	66.29	4.2	66.29	1.04384134	0.042907501	4
17	70.49	4.2	70.49	1.04384134	0.042907501	4.123105626
18	74.69	4.2	74.69	1.04384134	0.042907501	4.242640687
19	78.89	4.2	78.89	1.04384134	0.042907501	4.358898944
20	83.09	4.2	83.09	1.04384134	0.042907501	4.472135955
21	87.29	4.2	87.29	1.04384134	0.042907501	4.582575695
22	91.49	4.2	91.49	1.04384134	0.042907501	4.69041576
23	95.69	4.2	95.69	1.04384134	0.042907501	4.795831523
24	99.89	4.2	99.89	1.04384134	0.042907501	4.898979486

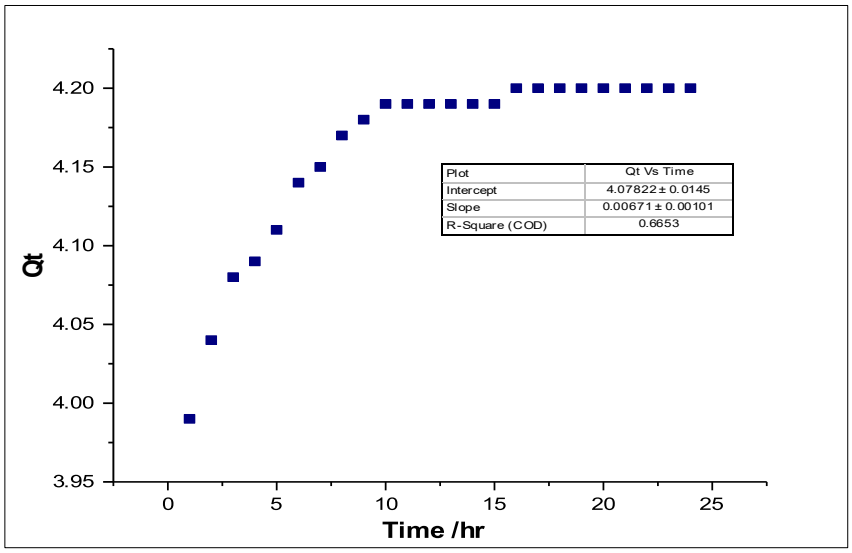

Figure (11) Zero-order kinetic model for the release of cephalexin from Gel/PEG into SIF

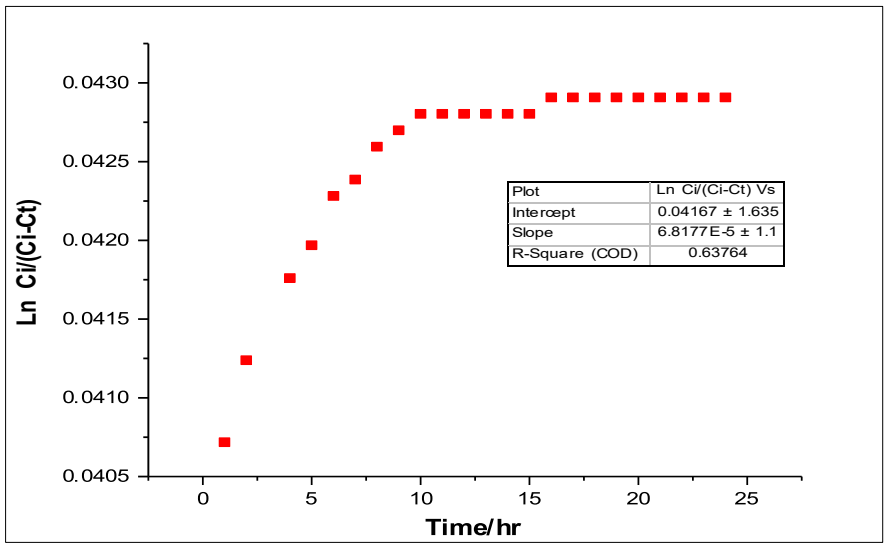

Figure (12) First-order kinetic model for the release of cephalexin from Gel/PEG into SIF

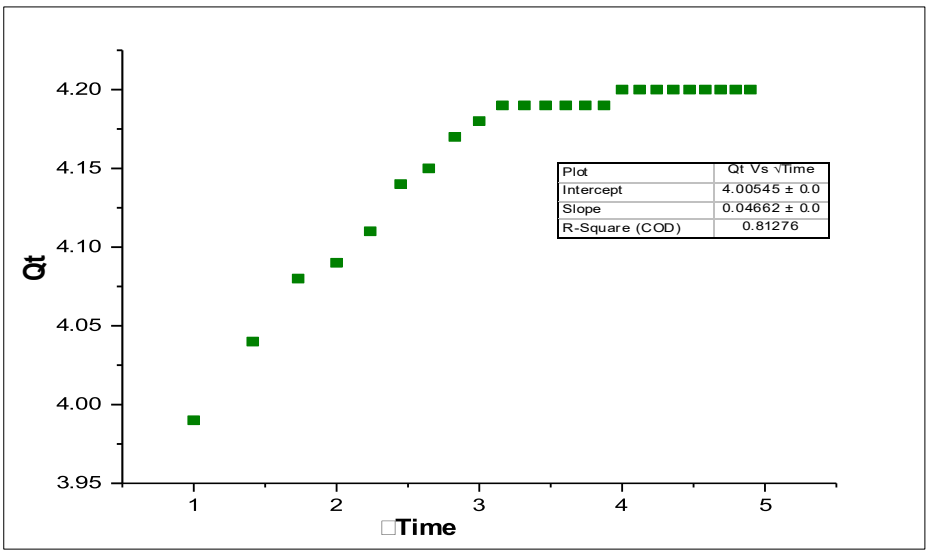

Figure (13) Higuchi-order kinetic model for the release of cephalexin from Gel/PEG into SIF

Table (5) Kinetic Parameters of Cephalexin Release from Gel/PEG Matrix in SGF

Time	Cumulative Drug Release (ppm)	Amount Released per Hour	Release%	First Order		Higuchi
		Qt	(Ct/Ci)*100%	Ci/(Ci-Ct)	Ln Ci/(Ci-Ct)	t^1/2
1	1.64	1.64	1.64	1.01667344	0.016535969	1
2	3.32	1.68	3.32	1.01708706	0.016942721	1.414213562
3	5.04	1.72	5.04	1.01750102		1.732050808
4	6.79	1.75	6.79	1.0178117	0.017654935	2
5	8.57	1.78	8.57	1.01812258	0.017960325	2.236067977
6	10.38	1.81	10.38	1.01843365	0.018265809	2.449489743
7	12.21	1.83	12.21	1.01864113	0.018469516	2.645751311
8	14.04	1.83	14.04	1.01864113	0.018469516	2.828427125
9	15.89	1.85	15.89	1.0188487	0.018673265	3
10	17.75	1.86	17.75	1.01895252	0.018775155	3.16227766
11	19.61	1.86	19.61	1.01895252	0.018775155	3.31662479
12	21.47	1.86	21.47	1.01895252	0.018775155	3.464101615
13	23.34	1.87	23.34	1.01905635	0.018877056	3.605551275
14	25.22	1.88	25.22	1.01916021	0.018978967	3.741657387
15	27.1	1.88	27.1	1.01916021	0.018978967	3.872983346
16	28.98	1.88	28.98	1.01916021	0.018978967	4
17	30.86	1.88	30.86	1.01916021	0.018978967	4.123105626
18	32.76	1.9	32.76	1.01936799	0.019182819	4.242640687
19	34.66	1.9	34.66	1.01936799	0.019182819	4.358898944
20	36.57	1.91	36.57	1.01947191	0.019284761	4.472135955
21	38.48	1.91	38.48	1.01947191	0.019284761	4.582575695
22	40.4	1.92	40.4	1.01957586	0.019386714	4.69041576
23	42.32	1.92	42.32	1.01957586	0.019386714	4.795831523
24	44.24	1.92	44.24	1.01957586	0.019386714	4.898979486

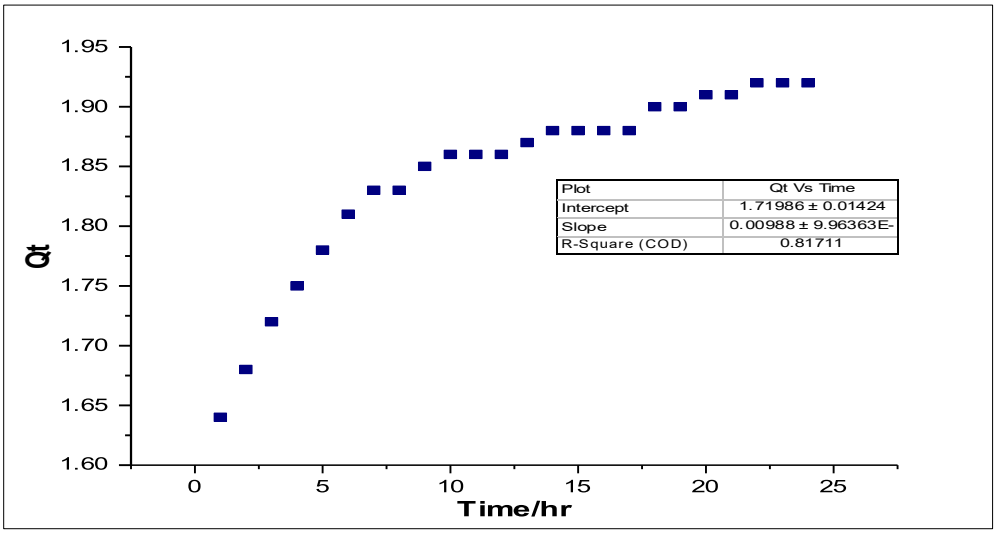

Figure (14) Zero-order kinetic model for the release of cephalexin from Gel/PEG into SGF

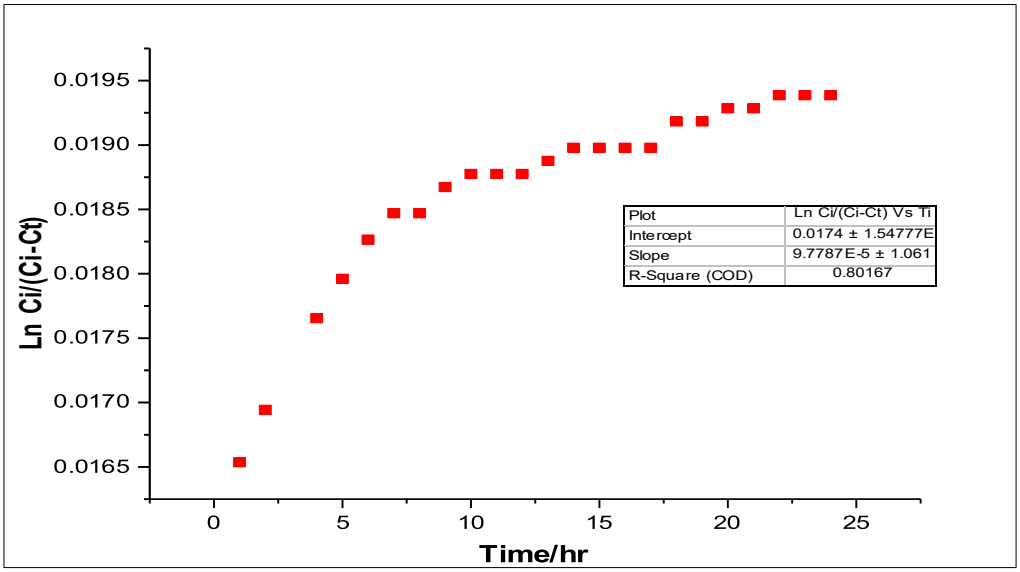

Figure (15) First-order kinetic model for the release of cephalexin from Gel/PEG into SGF

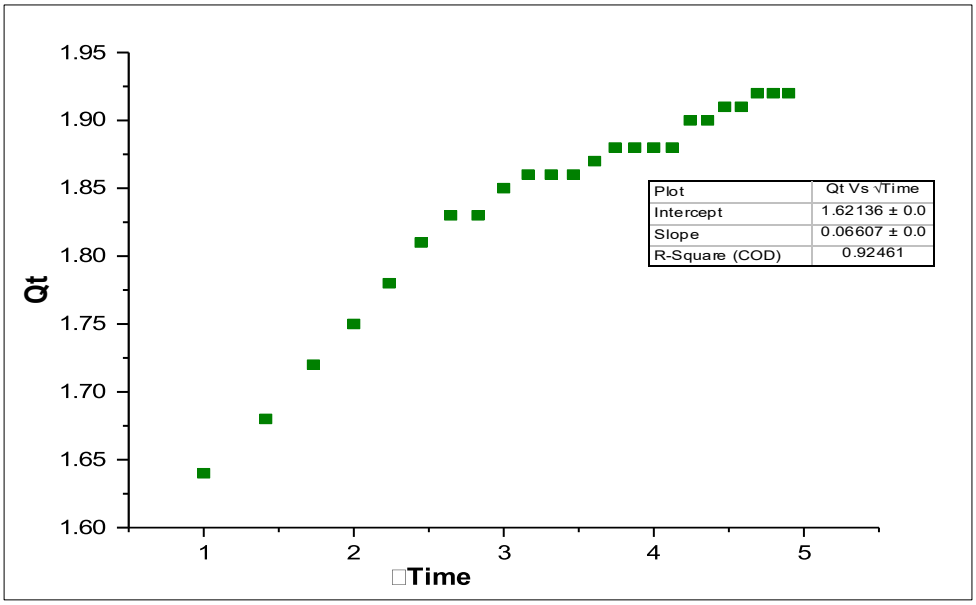

Figure (16) Higuchi-order kinetic model for the release of cephalexin from Gel/PEG into SGF

3.11 SEM Measurement for polymeric matrix

Scanning Electron Microscopy (SEM) was employed to evaluate the morphological characteristics of the Gel/PEG/ZnO polymeric matrix, both before and after the incorporation of the model antibiotic drug, cephalexin. Micrographs were obtained at a magnification scale of 200 nm to observe nanoscale surface features and morphological transitions resulting from drug loading. In the Gel/PEG matrix (Figure 17), the SEM images prior to drug loading show a smooth and moderately aggregated surface with minimal topographical complexity. Post-drug loading, the morphology becomes notably more heterogeneous, with observable crystalline formations, irregular particle shapes, and increased surface roughness. These structural transformations imply effective drug integration into the matrix via either surface entrapment or internal encapsulation mechanisms. Such morphological shifts serve as strong indicators of successful drug loading and suggest enhanced interaction between the polymer and the cephalexin molecules [36,37].

Overall, the pronounced morphological changes in the matrix at the nanoscale provide visual confirmation of drug incorporation and greatly support the functionality of Gel/PEG systems as potential candidates for controlled drug delivery platforms.

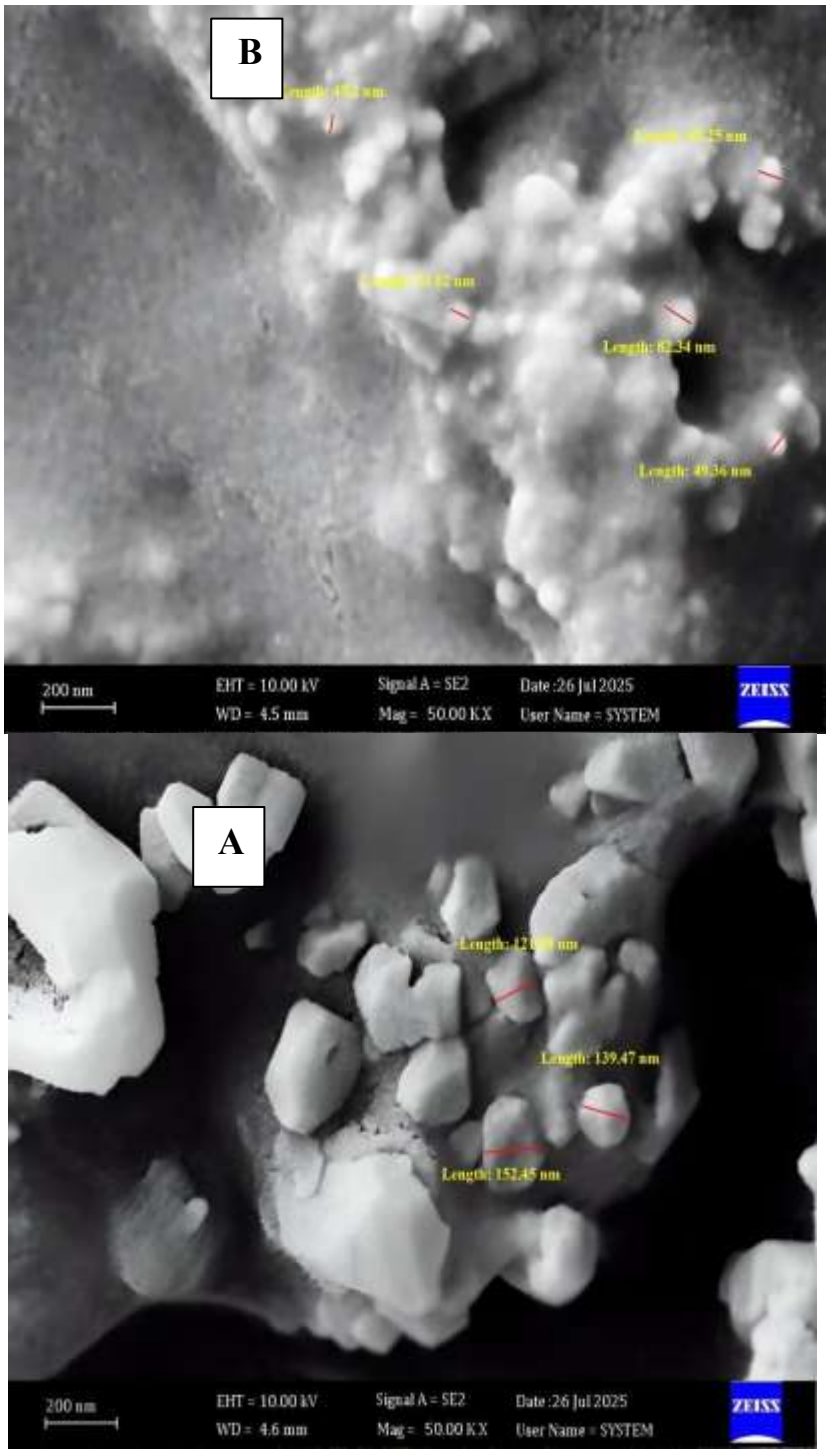

Figure (17). Scanning Electron Microscopy (SEM) micrographs of the Gel/PEG/ZnO polymer matrix at 200 nm magnification: (A) prior to drug loading (B) after drug loading

3.12 Antibacterial Activity Assessment of Gelatin-Based Polymeric Matrix

The antibacterial potential of gelatin-based nanocomposite systems was assessed using the agar well diffusion method, as illustrated in Figure 18. The antimicrobial evaluation focused on two bacterial strains: Staphylococcus aureus (Gram-positive) and Escherichia coli (Gram-negative). Three different sample formulations were prepared to examine the contribution of each component gelatin, polyethylene glycol (PEG), zinc oxide (ZnO) nanoparticles, and cephalexin toward antibacterial performance.

Bacterial suspensions were standardized to a concentration of 1.5×10^1 CFU/mL using sterile physiological saline and calibrated against the 0.5 McFarland turbidity standard for consistency. Mueller Hinton Agar (MHA) was autoclaved and poured into sterile Petri dishes under aseptic conditions. After

the surface of the agar was inoculated with the test organisms, wells were created using sterile cork borers, and 100 µL of each test formulation was introduced into the wells. Plates were incubated at 37°C for 24 hours, and the diameters of the zones of inhibition were measured in millimeters (mm) to determine antibacterial efficacy [38-41].

The formulations used in this study were:

1Gel: Gelatin + PEG + ZnO nanoparticles + Cephalexin

2Gel: Gelatin + PEG

3Gel: Gelatin + PEG + ZnO nanoparticles

The antimicrobial efficacy results are tabulated in Table 6:

Table (6) Inhibition zone diameters (mm) of gelatin-based nanocomposites against S. aureus and E. coli

	(S.a)	(E.c)
1Gel	**20**	-
2Gel	**13**	-
3Gel	**10**	-

As indicated in Table 6, antibacterial activity was only observed against S. aureus, with no inhibition recorded against E. coli. Among all samples, 1Gel exhibited the highest antibacterial effect, yielding a 20 mm inhibition zone. This can be attributed to the synergistic antibacterial mechanisms of ZnO nanoparticles and cephalexin. ZnO disrupts bacterial cell membranes and induces oxidative stress via reactive oxygen species (ROS), while cephalexin interferes with bacterial cell wall biosynthesis. Reduced inhibition in 2Gel and 3Gel underscores the necessity of both active agents for optimal antibacterial performance, as depicted in Figure 19.

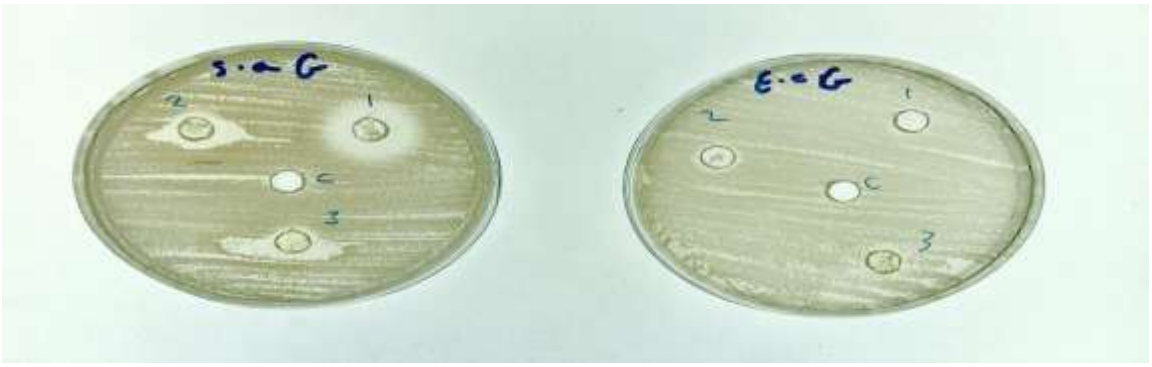

Figure (18) Antibacterial activity of gelatin-based polymeric nanocomposites against Staphylococcus aureus (left) and Escherichia coli (right) using the agar well diffusion method.

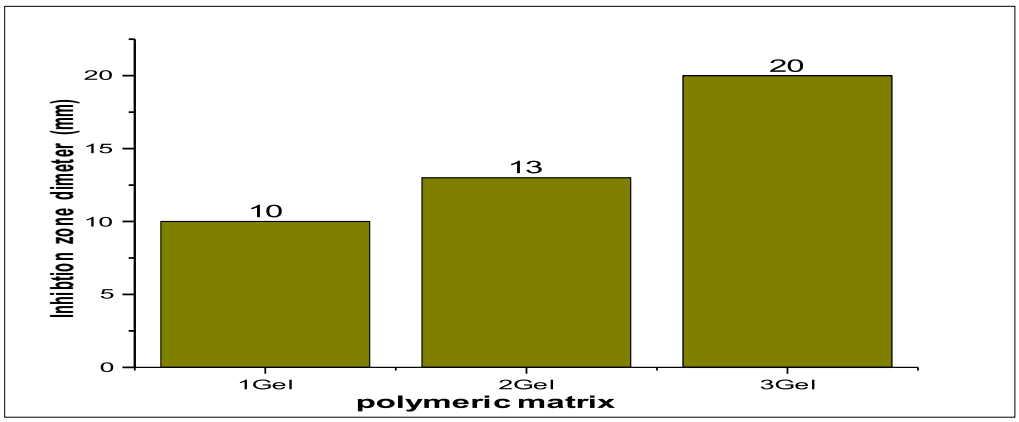

Figure (19) Comparative bar graph representing the inhibition zone diameters of gelatin-based samples against Staphylococcus aureus .

CONCLUSIONS

1. the polymeric nanocomposite matrix, Gel/PEG/ZnO, were successfully synthesized and crosslinked using glutaraldehyde.
2. FTIR spectroscopy confirmed the successful incorporation of cephalexin and highlighted key functional group interactions within the polymeric networks.
3. The swelling behavior of the matrix was pH-dependent, with Gel/PEG exhibiting greater swelling ratios, particularly in simulated intestinal fluid.
4. Drug release kinetics followed a predominantly diffusion-controlled mechanism, best described by the Higuchi model.
5. SEM analysis revealed significant surface morphological changes after drug loading, confirming successful encapsulation and interaction within the polymer structure.
6. Antibacterial testing demonstrated that the Gel/PEG/ZnO nanocomposite had enhanced activity against Staphylococcus aureus, attributed to the combined effect of ZnO nanoparticles and cephalexin.
7. Overall, the developed polymeric systems exhibit promising characteristics for use as controlled-release drug delivery platforms, particularly for oral antibiotic administration.

REFERENCES

1 C. O. Egwu et al., "Nanomaterials in Drug Delivery: Strengths and Opportunities in Medicine," Molecules, vol. 29, no. 11, 2024, doi: 10.3390/molecules29112584.
2 Y. H. Yun, B. K. Lee, and K. Park, "Controlled Drug Delivery: Historical perspective for the next generation," J. Control. Release, vol. 219, pp. 2–7, 2015, doi: 10.1016/j.jconrel.2015.10.005.
3 A. Ganesan, "The impact of natural products upon modern drug discovery," Curr. Opin. Chem. Biol., vol. 12, no. 3, pp. 306–317, 2008, doi: 10.1016/j.cbpa.2008.03.016.
4 A. Salimi, B. S. Makhmalzadeh, and G. Esfahani, "Polymeric Micelle as a New Carrier in Oral Drug Delivery Systems," Asian J. Pharm., vol. 11, no. 4, pp. 704–711, 2017.
5 K. Park, "Drug delivery research: The invention cycle," Mol. Pharm., vol. 13, no. 7, pp. 2143–2147, 2016, doi: 10.1021/acs.molpharmaceut.6b00015.
6 S. M. H. Ali, "Synthesis and Investigation of Hybrid Polyoxometalate (POM) -Dopamine Nano-Structures as Drug Delivery System," University of Kerbala, 2021.
7 M. Chandalia, A. Garg, D. Lutjohann, K. von Bergmann, S. M. Grundy, and L. J. Brinkley, "Beneficial Effects of High Dietary Fiber Intake in Patients with Type 2 Diabetes Mellitus," N. Engl. J. Med., vol. 342, no. 19, pp. 1392–1398, 2000, doi: 10.1056/nejm200005113421903.
8 G. Beccuti et al., "Timing of food intake: Sounding the alarm about metabolic impairments? A systematic review," Pharmacol. Res., vol. 125, pp. 132–141, 2017, doi: 10.1016/j.phrs.2017.09.005.
9 S. Mehra, S. Nisar, S. Chauhan, V. Singh, and S. Rattan, "Soy Protein-Based Hydrogel under Microwave-Induced Grafting of Acrylic Acid and 4-(4-Hydroxyphenyl)butanoic Acid: A Potential Vehicle for Controlled Drug Delivery in Oral Cavity Bacterial Infections," ACS Omega, vol. 5, no. 34, pp. 21610–21622, 2020, doi: 10.1021/acsomega.0c02287.
10 D. Verma, N. Gulati, S. Kaul, S. Mukherjee, and U. Nagaich, "Protein Based Nanostructures for Drug Delivery," J. Pharm., vol. 2018, pp. 1–18, 2018, doi: 10.1155/2018/9285854.
11 X. Jiang et al., "Gelatin-based anticancer drug delivery nanosystems: A mini review," Front. Bioeng. Biotechnol., vol. 11, no. March, pp. 1–7, 2023, doi: 10.3389/fbioe.2023.1158749.
12 R. M. Hathout, A. A. Metwally, T. J. Woodman, and J. G. Hardy, "Prediction of Drug Loading in the Gelatin Matrix Using Computational Methods," ACS Omega, vol. 5, no. 3, pp. 1549–1556, 2020, doi: 10.1021/acsomega.9b03487.
13 H. S. Mahdi and S. M. Alshrefi, "pH-Sensitive Swelling Behavior and Drug Release Kinetics of Chitosan-Modified Cs/HEMA Hydrogels," pp. 1–20, 2024, [Online]. Available: https://www.researchsquare.com/article/rs-3978283/v1
14 N. Yacob and K. Hashim, "Morphological effect on swelling behaviour of hydrogel," AIP Conf. Proc., vol. 1584, no. November 2016, pp. 153–159, 2014, doi: 10.1063/1.4866123.
15 K. Afriani, S. Suhartini, and G. Maulia, "Synthesis and Characterization of Hydrogel Alginate/Poly (N-Vinyl -2-Pyrrolidone) with Double Ionic Cross-Bonded for Drug Delivery and Antibacterial Agent," Egypt. J. Chem., vol. 67, no. 2, pp. 205–213, 2024, doi: 10.21608/EJCHEM.2023.209529.7949.
16 D. Ramesh, S. M. Bakkannavar, V. R. Bhat, K. S. R. Pai, and K. Sharan, "Correction to: Comparative study on drug encapsulation and release kinetics in extracellular vesicles loaded with snake venom L - amino acid oxidase (BMC Pharmacology and Toxicology, (2025), 26, 1, (98), 10.1186/s40360-025-00938-8)," BMC Pharmacol. Toxicol. , vol. 26, no. 1, 2025, doi: 10.1186/s40360-025-00956-6.
17 Y. Yao, X. Gao, and Z. Zhou, "The application of drug loading and drug release characteristics of two-dimensional nanocarriers for targeted treatment of leukemia," Front. Mater., vol. 10, no. June, pp. 1–13, 2023, doi: 10.3389/fmats.2023.1209186.
18 N. H. Jamalludin and N. A. Tukiran, "Analysis of gelatin adulteration in edible bird's nest using Fourier transform infrared (FTIR) spectroscopy," Int. J. Adv. Sci. Eng. Inf. Technol., vol. 8, no. 6, pp. 2355–2359, 2018, doi: 10.18517/ijaseit.8.6.7690.
19 D. N. Mustaqimah and A. P. Roswiem, "Identification of Gelatin in Dental Materials using the Combination of Attenuated Total Reflection-Fourier Transform Infrared Spectroscopy (ATR-FTIR) and Chemometrics," Int. J. Halal Res., vol. 2, no. 1, pp. 1–15, 2020, doi: 10.18517/ijhr.2.1.1-15.2020.
20 A. R. Polu and R. Kumar, "Impedance spectroscopy and FTIR studies of PEG - Based polymer electrolytes," E-Journal Chem., vol. 8, no. 1, pp. 347–353, 2011, doi: 10.1155/2011/628790.

21 S. Roy, D. Biswas, and J. W. Rhim, "Gelatin/Cellulose Nanofiber-Based Functional Nanocomposite Film Incorporated with Zinc Oxide Nanoparticles," J. Compos. Sci., vol. 6, no. 8, pp. 1–11, 2022, doi: 10.3390/jcs6080223.
22 X. Feng et al., "Food-grade gelatin nanoparticles: Preparation, characterization, and preliminary application for stabilizing pickering emulsions," Foods, vol. 8, no. 10, 2019, doi: 10.3390/foods8100479.
23 D. Leila, L. G. Mar, B. Fatima, N. Abddelyamine, B. Ali, and H. Nacereddine, "Effect of polyethylene glycol and propyltrimethoxysilane on structural and optical properties of zinc oxide nanoparticles synthesized by sol–gel process," J. Theor. Appl. Phys., vol. 12, no. 3, pp. 159–167, 2018, doi: 10.1007/s40094-018-0303-2.
24 & R. Bigi, A., Cojazzi, G., Panzavolta, S., Rubini, K., "Mechanical and thermal properties of gelatin films at different degrees of glutaraldehyde crosslinking," Biomaterials, vol. 22, no. 8, pp. 763–768, 2001.
25 I. México Martínez-Vázquez et al., "Universidad Autónoma Metropolitana Unidad Swelling kinetic of hydrogels from methyl cellulose and poly (acrylamide) Revista Mexicana de Ingeniería SWELLING KINETIC OF HYDROGELS FROM METHYL CELLULOSE AND POLY(ACRYLAMIDE) CINÉTICA DE HINCHAMIENTO DE HIDROGE," México Rev. Mex. Ing. QUÍMICA, vol. 6, no. 3, pp. 337–345, 2007, [Online]. Available: http://www.redalyc.org/articulo.oa?id=62060313
26 E. Fagir, W., Hathout, R. M., Sammour, O. A., "Self-microemulsifying systems of Finasteride with enhanced oral bioavailability: multivariate statistical evaluation, characterization, spray-drying and in vivo studies in human volunteers," Nanomedicine, vol. 10, no. 22, pp. 3373–3389, 2015.
27 H. Schott, "Kinetics of swelling of polymers and their gels," Pharm. Sci., vol. 81, no. 5, pp. 467–470, 1992.
28 N. Bouklas and R. Huang, "Swelling kinetics of polymer gels: Comparison of linear and nonlinear theories," Soft Matter, vol. 8, no. 31, pp. 8194–8203, 2012, doi: 10.1039/c2sm25467k.
29 A. K. Kurzeck, B. Kirsch, E. Weidinger, F. Padberg, and U. Palm, "Transcranial direct current stimulation (tDCS) for depression during pregnancy: Scientific evidence and what is being said in the media—a systematic review," Brain Sci., vol. 8, no. 8, 2018, doi: 10.3390/brainsci8080155.
30 S. Nangia, D. Katyal, and S. Warkar, "Kinetics, absorption and diffusion mechanism of crosslinked Chitosan Hydrogels," Indian J. Eng. Mater. Sci., vol. 28, no. 4, pp. 374–384, 2021, doi: 10.56042/ijems.v28i4.44361.
31 F. Ganji, S. Vasheghani-Farahani, and E. Vasheghani-Farahani, "Theoretical description of hydrogel swelling: A review," Iran. Polym. J. (English Ed., vol. 19, no. 5, pp. 375–398, 2010.
32 M. E. A. Mohsin, A. J. Siddiqa, S. Mousa, and N. K. Shrivastava, "Design, Characterization, and Release Kinetics of a Hybrid Hydrogel Drug Delivery System for Sustained Hormone Therapy," Polymers (Basel)., vol. 17, no. 8, 2025, doi: 10.3390/polym17080999.
33 M. A. Mohammed, J. T. M. Syeda, K. M. Wasan, and E. K. Wasan, "An Overview of Chitosan Nanoparticles and Its Application in Non-Parenteral Drug Delivery," 2017, doi: 10.3390/pharmaceutics9040053.
34 M. Bahram, N. Mohseni, and M. Moghtader, "An Introduction to Hydrogels and Some Recent Applications World ' s largest Science , Technology & Medicine Open Access book publisher," no. August, 2016, doi: 10.5772/64301.
35 N. Mahmoudi Khatir and A. Khorsand Zak, "Antibacterial activity and structural properties of gelatin-based sol-gel synthesized Cu-doped ZnO nanoparticles; promising material for biomedical applications," Heliyon, vol. 10, no. 17, p. e37022, 2024, doi: 10.1016/j.heliyon.2024.e37022.
36 Y. C. Yu, M. H. Hu, H. Z. Zhuang, T. H. M. Phan, Y. S. Jiang, and J. S. Jan, "Antibacterial Gelatin Composite Hydrogels Comprised of In Situ Formed Zinc Oxide Nanoparticles," Polymers (Basel)., vol. 15, no. 19, 2023, doi: 10.3390/polym15193978.
37 H. M. Al-Asadi, S. A. Obaid, and R. A. Ghazi, "Enhanced Optical and Structural Properties of ZnO NPs Doped PVA/PEG/PVP and its Use in Bacterial Activity," *Instrum. Mes. Metrol.*, vol. 24, no. 1, pp. 89–95, 2025, doi: 10.18280/i2m.240110.
38 Y. Chen, W. Lu, Y. Guo, Y. Zhu, and Y. Song, "Electrospun gelatin fibers surface loaded ZnO particles as a potential biodegradable antibacterial wound dressing," Nanomaterials, vol. 9, no. 4, 2019, doi: 10.3390/nano9040525.
39 F. D. Gonelimali et al., "Antimicrobial properties and mechanism of action of some plant extracts against food pathogens and spoilage microorganisms," Front. Microbiol., vol. 9, no. JUL, pp. 1–9, 2018, doi: 10.3389/fmicb.2018.01639.
40 S. T. Sadiq and H. Yildirim, "Antibacterial, Antifungal, Antioxidant Activities Assessment Of Some Newly Registered Plant Extracts Collected From Izmir City," Recent Adv. Biol. Med., vol. 10, 2024, doi: 10.18639/rabm.2024.9800041.
41 M. Balouiri, M. Sadiki, and S. K. Ibnsouda, "Methods for in vitro evaluating antimicrobial activity: A review," J. Pharm. Anal., vol. 6, no. 2, pp. 71–79, 2016, doi: 10.1016/j.jpha.2015.11.005.